*Supporting information*

# Thermoplastic charge-transfer hydrogels for highly sensitive strain and temperature sensors

***Ru Zhang,*[†] *Cuiwen Liu,*[†] *Chengmeng Wei,*[†] *Yao Wang,*[†] *Feng Li,*[†] *Zhiqiang Zhang,*[†] *Jinqing Qu,*[‡] *Ning Qing,*[†] *Liuyan Tang*[*, †]**

[†]School of Biotechnology and Health Sciences, Wuyi University, Jiangmen, 529020, China

[‡]School of Chemistry and Chemical Engineering, South China University of Technology, Guangzhou 510640, China

*Corresponding author.

E-mails: wyuchemtangly@126.com (Liuyan Tang).

**Table S1.** Compositions of CT-K hydrogels.

| Sample | MVBBP (mg) | SVBPTS (mg) | NaSS (mg) | $H_2O$ (mL) | ACVA (mg) | KCl (mg) |
|---|---|---|---|---|---|---|
| $CT_1$-$K_0$ | 61.7 | 88.0 | 296.9 | 1.2 | 4.8 | / |
| $CT_1$-$K_{0.3}$ | 61.7 | 88.0 | 296.9 | 1.2 | 4.8 | 26.8 |
| $CT_1$-$K_{0.5}$ | 61.7 | 88.0 | 296.9 | 1.2 | 4.8 | 44.7 |
| $CT_1$-$K_{0.7}$ | 61.7 | 88.0 | 296.9 | 1.2 | 4.8 | 62.6 |
| $CT_1$-$K_1$ | 61.7 | 88.0 | 296.9 | 1.2 | 4.8 | 89.5 |
| $CT_1$-$K_{1.3}$ | 61.7 | 88.0 | 296.9 | 1.2 | 4.8 | 116.3 |
| $CT_1$-$K_{1.5}$ | 61.7 | 88.0 | 296.9 | 1.2 | 4.8 | 134.2 |
| $CT_2$-$K_1$ | 136.5 | 97.3 | 296.9 | 1.2 | 5.2 | 89.5 |
| $CT_3$-$K_1$ | 228.7 | 108.7 | 296.9 | 1.2 | 5.8 | 89.5 |

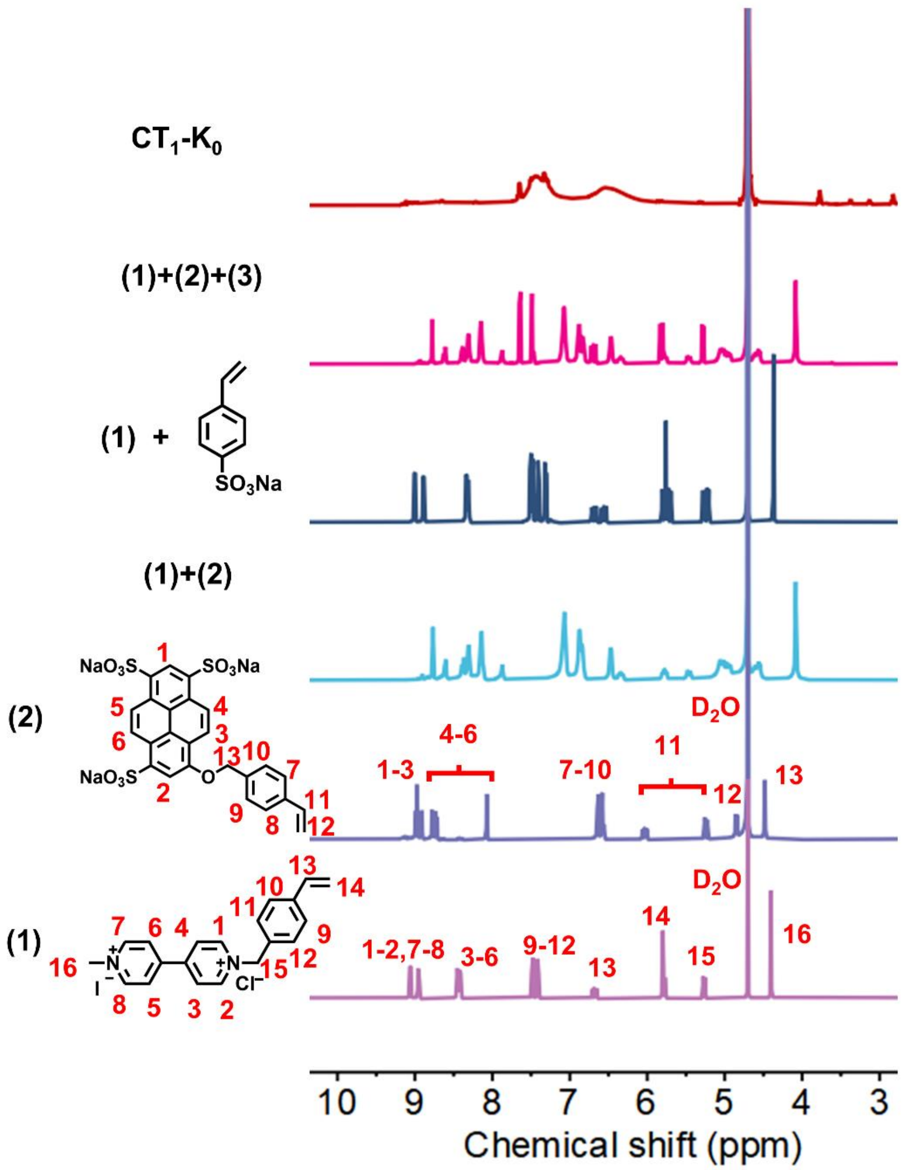


**Fig.S1** The [1]H NMR spectra of MVBBP, SVBPTS, the mixture of MVBBP and SVBPTS, the mixture of MVBBP and NaSS, the mixture of MVBBP, SVBPTS and NaSS, and the diluted solution of $CT_1$-$K_0$ hydrogel using $D_2O$ as solvent.

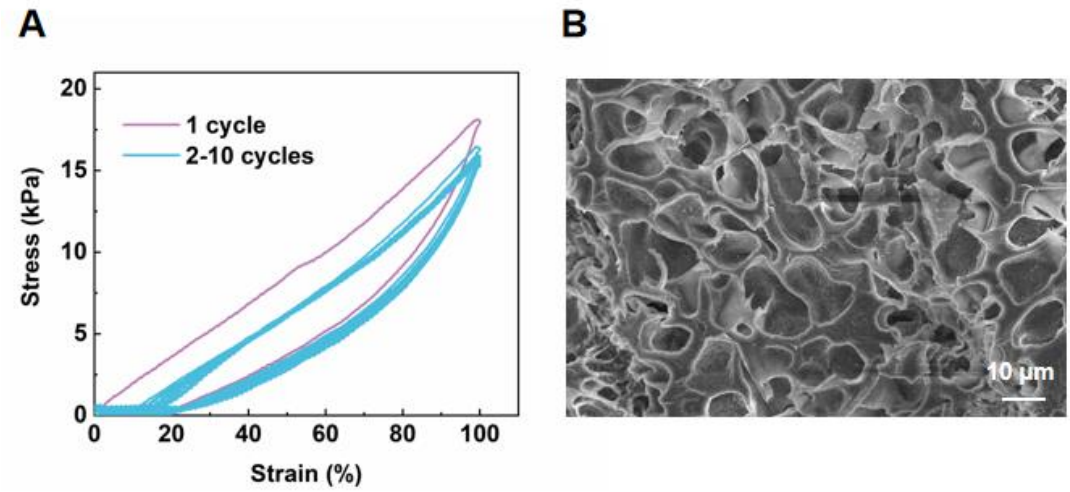


**Fig.S2** (A) The cyclic loading–unloading curves of the $CT_1$-$K_1$ hydrogel at a strain of 100% for 10 cycles. (B) The SEM images of the $CT_1$-$K_1$ hydrogel after being stretched at a strain of 100% for 10 cycles.

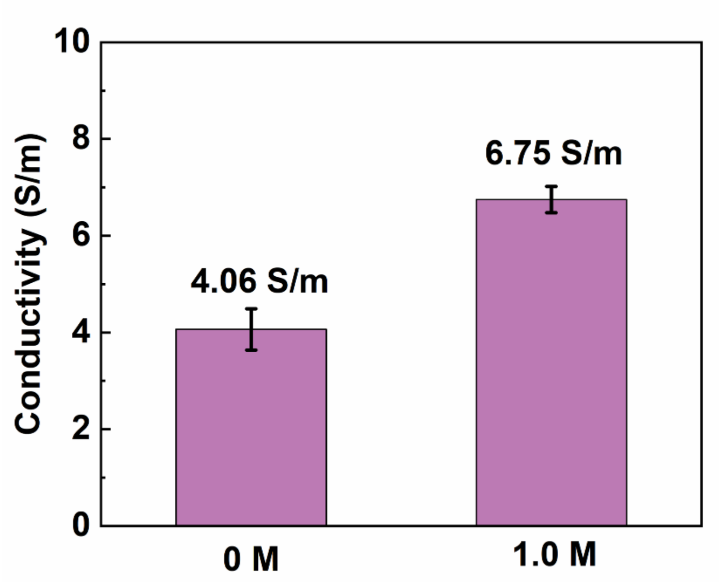


**Fig.S3** The conductivity of $CT_1$-$K_0$ and $CT_1$-$K_1$ hydrogels.

**Table S2.** A comparison on the gauge factor and strain sensing range of the strain sensor in this work with other hydrogel-based strain sensors.

| Sensing materials | Gauge factor | Strain ranges (%) | Ref. |
|---|---|---|---|
| starch/polyacrylamide/borax/glycerol | 0.87<br>1.47 | 0-230<br>230-500 | 1 |
| Cellulose/PA/PANI | 2.62 | 0-120 | 2 |
| TAPU/Fe-4 hydrogel | 1.73<br>2.15<br>3.24 | 0-40<br>40-100<br>100-200 | 3 |
| PAA/NCT hydrogel | 2.69 | 0-500 | 4 |
| PAM/CC/NaCl gel | 0.104<br>0.214 | 0.5-300<br>300-800 | 5 |
| P(SBMA-co-AAc)/CS-Cit DN hydrogel | 2.93 | 0-150 | 6 |
| PVA/PA/NP-2 hydrogel | 3.44 | 0-125 | 7 |
| PBST4 sensor<br>(PVA, borax, SF, and TA) | 1.66 | -650 | 8 |
| $PC_{4.5}T_6M_{45}$-3 hydrogel | 2.9 | 0-700 | 9 |
| $PGS_8C_{2.0}$ hydrogel | 1.54<br>2.32<br>2.68 | 0-100<br>200-300<br>400-500 | 10 |
| $CT_1$-$K_1$ | 4.02<br>8.71 | 0-350<br>350-900 | This work |

**Table S3.** A comparison on the TCR and temperature sensing range of the temperature sensor in this work with other temperature sensors.

| **Sensing materials** | **TCR (% °C$^{-1}$)** | **Temperature ranges (°C)** | **Ref.** |
|---|---|---|---|
| PGBC-B organohydrogel | 0.956 | 30-90 | 11 |
| BP/LEG on SEBS | 0.1736 | 25-50 | 12 |
| LC-GO/CMC | 0.289 | 20-80 | 13 |
| Laser-engraved graphene | 0.06 | 25-50 | 14 |
| Ag nanocrystal/PDMS | 0.185 | 30-50 | 15 |
| N, F-CDs | 1.11 | 25-60 | 16 |
| interlocked TPU@IL2 | 2.10<br>0.62<br>0.57 | 30-50<br>50-77<br>77-98 | 17 |
| 3 wt% Composites | 0.8 | 20-65 | 18 |
| PTCF | 0.95 | 20-40 | 19 |
| laser-patterned carbonized films | 0.142 | -10-60 | 20 |
| $CT_1$-$K_1$ | 3.20<br>1.39<br>0.72 | 5-20<br>20-50<br>50-70 | This work |

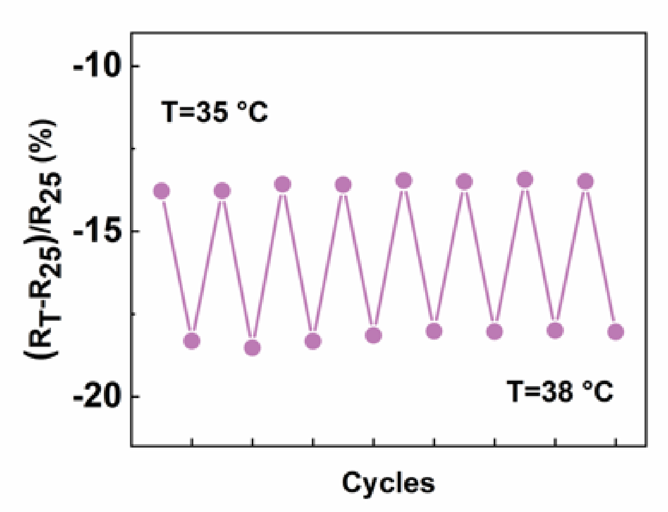


**Fig.S4** Repetitive temperature-discrimination ability of $CT_1$-$K_1$ hydrogel-based temperature sensor by alterative placing at 35 °C and 38 °C.

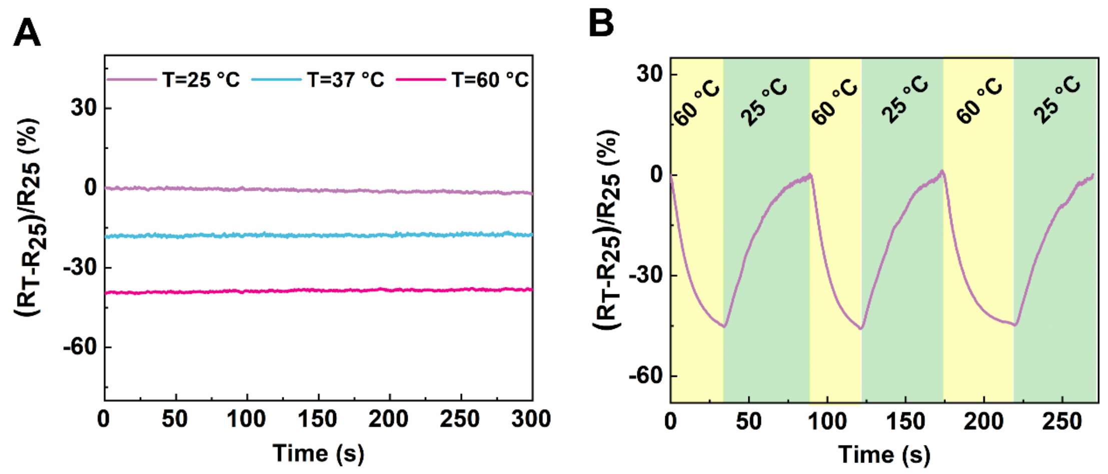


**Fig.S5** (A) Resistance stability test of $CT_1$-$K_0$ hydrogel-based temperature sensor at 25 ℃, 37 ℃ and 60 ℃. (B) The instantaneous electrical response of $CT_1$-$K_0$ hydrogel-based temperature sensor by alterative placing at high (60 °C) and low (25 °C) temperature.

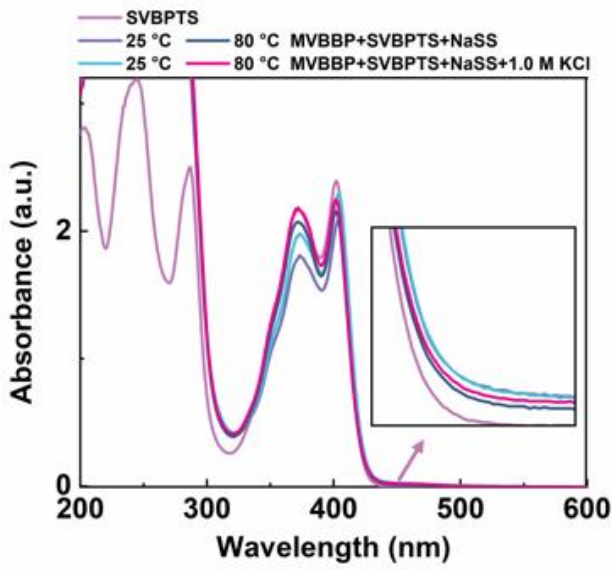


**Fig.S6** The UV-Vis spectra of the mixed solution of MVBBP, SVBPTS and NaSS with or without 1 M KCl at 25 °C and 80 °C.

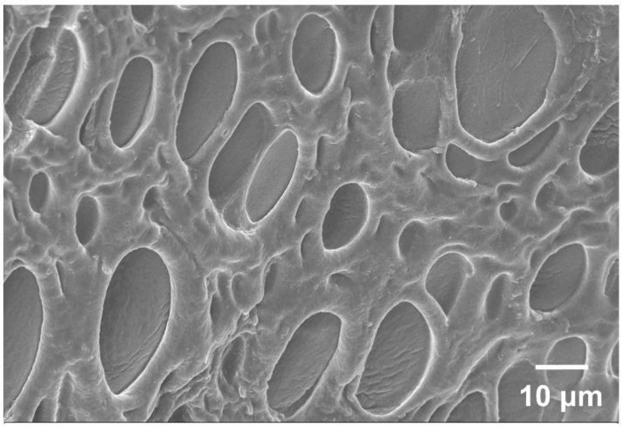


**Fig.S7** The SEM image of the thermoplastic $CT_1$-$K_1$ hydrogel.

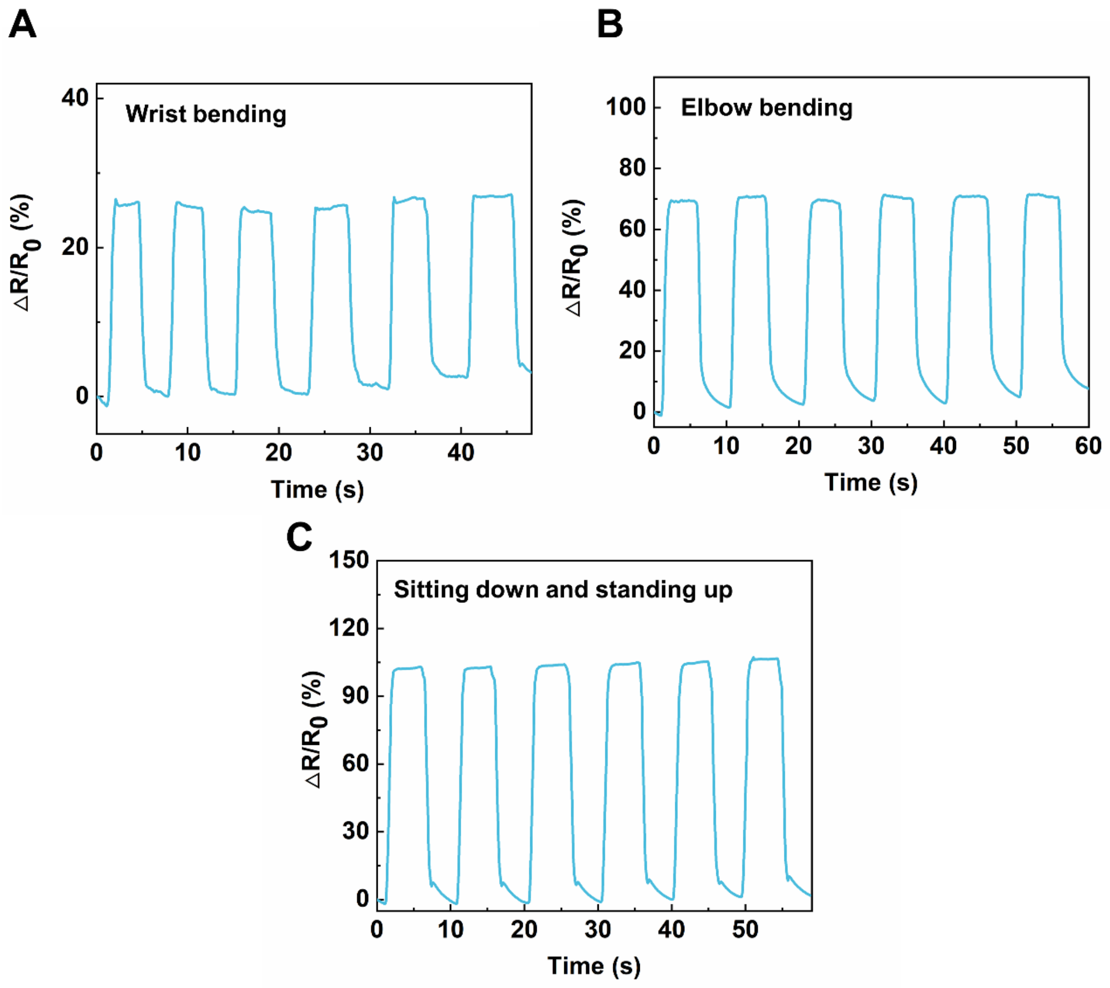


**Fig.S8** Application of the thermoplastic $CT_1$-$K_1$ hydrogel-based sensor in monitoring (A) Wrist bending. (B) Elbow bending. (C) Sitting down/standing up.

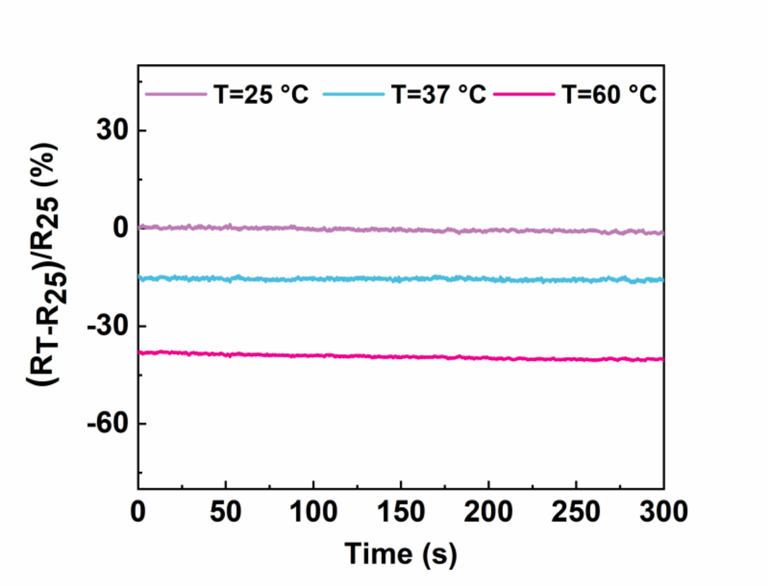


**Fig.S9** Resistance stability test of thermoplastic $CT_1$-$K_1$ hydrogel-based temperature sensor at 25 °C, 37 °C and 60 °C.

**References:**

1 W. Si, Y. Liang, Y. Chen and S. Zhang, *J. Mater. Chem. A*, 2022, **10**, 17464–17476.

2 H. Wan, C. Qin and A. Lu, *J. Mater. Chem. A*, 2022, **10**, 17279–17287.

3 Y. Liu, Z. Zhang, Z. Liang, Y. Yong, C. Yang and Z. Li, *J. Mater. Chem. A*, 2022, **10**, 16928–16940.

4 X. Jing, P. Feng, Z. Chen, Z. Xie, H. Li, X. F. Peng, H. Y. Mi and Y. Liu, *ACS Sustain. Chem. Eng.*, 2021, **9**, 9209–9220.

5 H. Ding, X. Liang, Q. Wang, M. Wang, Z. Li and G. Sun, *Carbohydr. Polym.*, 2020, **248**, 116797.

6 J. Zhang, L. Chen, B. Shen, Y. Wang, P. Peng, F. Tang and J. Feng, *Mater. Sci. Eng. C*, 2020, **117**, 111298.

7 L. Shao, Y. Li, Z. Ma, Y. Bai, J. Wang, P. Zeng, P. Gong, F. Shi, Z. Ji, Y. Qiao, R. Xu, J. Xu, G. Zhang, C. Wang and J. Ma, *ACS Appl. Mater. Interfaces*, 2020, **12**, 26496–26508.

8 H. Zheng, N. Lin, Y. He and B. Zuo, *ACS Appl. Mater. Interfaces*, 2021, **13**, 40013–40031.

9 D. Kong, Z. M. El-Bahy, H. Algadi, T. Li, S. M. El-Bahy, M. A. Nassan, J. Li, A. A. Faheim, A. Li, C. Xu, M. Huang, D. Cui and H. Wei, *Adv. Compos. Hybrid Mater.*, 2022, 1976–1987.

10 X. Liu, Z. Wu, D. Jiang, N. Guo, Y. Wang, T. Ding and L. Weng,

*Adv. Compos. Hybrid Mater.*, 2022, 1712–1729.

11 J. Gu, J. Huang, G. Chen, L. Hou, J. Zhang, X. Zhang, X. Yang, L. Guan, X. Jiang and H. Liu, *ACS Appl. Mater. Interfaces*, 2020, **12**, 40815–40827.

12 A. Chhetry, S. Sharma, S. C. Barman, H. Yoon, S. Ko, C. Park, S. Yoon, H. Kim and J. Y. Park, *Adv. Funct. Mater.*, 2021, **31**, 2170068.

13 Q. Li, R. Bai, Y. Gao, R. Wu, K. Ju, J. Tan and F. Xuan, *ACS Appl. Mater. Interfaces*, 2021, **13**, 10171–10180.

14 Y. Yang, Y. Song, X. Bo, J. Min, O. S. Pak, L. Zhu, M. Wang, J. Tu, A. Kogan, H. Zhang, T. K. Hsiai, Z. Li and W. Gao, *Nat. Biotechnol.*, 2020, **38**, 217–224.

15 J. Bang, W. S. Lee, B. Park, H. Joh, H. K. Woo, S. Jeon, J. Ahn, C. Jeong, T. il Kim and S. J. Oh, *Adv. Funct. Mater.*, 2019, **29**, 1–8.

16 J. Zhu, H. Chu, J. Shen, C. Wang and Y. Wei, *J. Colloid Interface Sci.*, 2021, **586**, 683–691.

17 Y. Xu, L. Chen, J. Chen, X. Chang and Y. Zhu, *ACS Appl. Mater. Interfaces*, 2022, **14**, 2122–2131.

18 L. Dan and A. L. Elias, *Adv. Healthc. Mater.*, 2020, **9**, 1–13.

19 F. Li, H. Xue, X. Lin, H. Zhao and T. Zhang, *ACS Appl. Mater. Interfaces*, 2022, **14**, 43844–43852.

20 S. Gandla, M. Naqi, M. Lee, J. J. Lee, Y. Won, P. Pujar, J. Kim, S. Lee and S. Kim, *Adv. Mater. Technol.*, 2020, **5**, 1–9.